

Automated Image Analysis in Multispectral System for Cervical Cancer Diagnostic

Natalia A. Obukhova, Alexandr A. Motyko
Saint Petersburg State Electro technical University LETI
Saint-Petersburg, Russia
natalia172419, motyko.alexandr@yandex.ru

Uk Kang, Soo-Jin Bae, Dae-Sic Lee
Korean Electrotechnology Research Institute
Seoul, Republic of Korea

Abstract—Uterine cervical cancer is the second most common cancer in women worldwide. The accuracy of colposcopy is highly dependent on the physicians individual skills. In expert hands, colposcopy has been reported to have a high sensitivity (96%) and a low specificity (48%) when differentiating abnormal tissues. This leads to a significant interest to activities aimed at the new diagnostic systems and new automatic methods of colposcopic images analysis development. The presented paper is devoted to developing method based on analyses fluorescents images obtained with different excitation wavelength. The sets of images were obtained in clinic by multispectral colposcope LuxCol. The images for one patient includes: images obtained with white light illumination and with polarized white light; fluorescence image obtained by excitation at wavelength of 360nm, 390nm, 430nm and 390nm with 635 nm laser. Our approach involves images acquisition, image processing, features extraction, selection of the most informative features and the most informative image types, classification and pathology map creation. The result of proposed method is the pathology map - the image of cervix shattered on the areas with the definite diagnosis such as norm, CNI (chronic nonspecific inflammation), CIN(cervical intraepithelial neoplasia). The obtained result on the border CNI/CIN sensitivity is 0.85, the specificity is 0.78. Proposed algorithms gives possibility to obtain correct differential pathology map with probability 0.8. Obtained results and classification task characteristics shown possibility of practical application pathology map based on fluorescents images.

I. INTRODUCTION

In 2002, 12285 cases of cervical cancer took place in Russia and in the Republic of Korea from 1993 to 2002, 44182 cases were diagnosed [1]. Cervical intra-epithelial neoplasia (CIN) is usually detected by means of screening Pap smears from asymptomatic women. Patients with abnormal Pap smears are referred for colposcopy and possibly biopsy. The purpose of a colposcopic examination is to identify and rank the severity of lesions, so that biopsies representing the highest-grade abnormality can be taken, if necessary. During colposcopy, 3-5% acetic acid solution is applied to the cervix, and areas with abnormal epithelium turn white. The colposcope is used to direct biopsies of the abnormal white areas. Additional lesion characteristics such as margin shape; color or opacity; blood vessel caliber, inter-capillary spacing and distribution are considered by physicians to derive a diagnosis.

The Pap smear and colposcopy have reduced both the incidence and mortality of cervical cancer [2]. But the Pap smear is a relatively simple test, it has been reported to have false positive errors at the rate of 15-40% [3], leading to a large number of unnecessary colposcopies. The accuracy of colposcopy is

highly dependent on the physician's individual skills. In expert hands, colposcopy has been reported to have a high sensitivity (96%) and a low specificity (48%) when differentiating abnormal tissues [3]. Because of the low specificity, a biopsy is required to confirm disease. These avoidable biopsies cause an increased risk of infection, patient discomfort, delayed treatment and substantially increased costs. There is a need for more objective, specific, and cost-effective screening and diagnostic techniques that could improve the accuracy of real-time detection, particularly in the hands of less-experienced practitioners. This leads to a significant number of activities aimed at the new diagnostic systems development. These system realized automatic image analysis of cervix, obtained in the white light illumination and fluorescence images. Image processing and computer vision technology are one of the key technologies to segment colposcopic images and detect cervical neoplasias.

Various image processing algorithms have been developed to detect different colposcopic features. Yang et al., at Texas Tech University, developed a segmentation algorithm to detect acetowhite epithelium using a statistical optimization scheme for accurate clustering to track the boundaries of the acetowhite regions [4]. J. Xiong et al. at Institute of Biomedical and Health Engineering, Shenzhen, China detected acetowhite regions on the base of chromaticity with watershed algorithm [5]. Huang et al. decided the task of acetowhite region detecting with color and brightness feature estimated in system Lab and HSV [6]. Gordon and coworkers, at Tel-Aviv University, developed a segmentation algorithm for three tissue types in cervical imagery (original squamous, columnar, and acetowhite epithelium) based on color and texture information [7]. The set of regions in the images was represented by a Gaussian mixture model, while an Expectation-Maximization algorithm was used to determine the maximum likelihood parameters of the statistical model in the feature space. As a result, the labeling of a pixel could be affiliated with the most probable Gaussian cluster according to Bayes rule. Ji et al [8], [9] presented a generalized texture analysis algorithm for classifying the vascular patterns from colposcopic images. They investigated six characteristic pathological vascular patterns, including network capillaries, hairpin capillaries, two types of punctation vessels and two types of mosaic vessels. Balas [10] and Orfanoudaki et al [11] analyzed the temporal decay of the acetic acid whitening effect by measuring the intensity profile over time.

Furthermore, several approaches for tissue classification

have been developed: a rule based medical decision support system for detecting different stages of cervical cancer based on the signs and symptoms from physical examination [12], [13], multivariate stochastic training algorithms [14]. All these methods and systems analyzed images obtained in the white light illumination. One of the promising and rapidly developing areas today is the multi-spectral diagnostic systems development. An example of a multi-spectral system is a device MDC (multi-spectral digital colposcope), developed at the University of Texas (USA), by the team of researchers led by R. Richards-Kortum [15], [16], [17]. Multi-spectral systems allow to get the new types of images. Fluorescent images contain additional diagnostic information based on the changes of concentration and restructuring endogenous fluorophores such as NADH, FAD, collagen, keratin, PPIX.

The presented paper is devoted to developing method based on analyses fluorescent images obtained with different excitation wavelength. Our investigation includes selection of informative features in the image of different types, their quantitative estimation, the estimation of different fluorescent images effectiveness and the development of specific analysis methods in order to identify the pathology area. We design approach includes analyses of different images type with the aim to get more information about changes in cervix tissue.

For improving results we used powerful classification strategy Random Decision Forest, instead Mahalanobis distance traditionally applied in fluorescent image analysis [18]. This method belongs to the group of data mining methods and its application is determined with the high degree of initial images variability (medical images from different patients have significant differences not only due to pathology, but due to the differences in age and other features of physical condition).

The main advantage of proposed method is new classification border realizing. In the most part of works the border is between normal tissue and tissue with CIN. But in the medicine practice the most interest is the determining difference between tissue with CIN (cervical intra-epithelial neoplasia) and CNI (chronic nonspecific inflammation). It should be noted that the state of tissues CNI and CIN I are very similar in their visual properties and making the choice between CNI and CIN I is not only the most important, but the most difficult problem during the colposcopic examination. The using more information obtained from images of different type and applying more complete and appropriate to task specificity classification strategy gives us possibility to develop the method realizing the differential diagnostic including three classes Norm, CNI, CIN. The result of proposed method is pathology map creation. Pathology map is the image of cervix shattered on the areas with the definite diagnosis such as norm, CNI, CIN. The presented paper includes a functional description of the multi-spectral colposcopic system LuxCol, algorithms for image analysis and results of our preliminary clinical research, which were carried out in the hospitals of South Korea, Seoul.

II. METHOD

A. Multispectral digital colposcope

The LuxCol consists of illuminator, multi-spectral image recorder unit, software and computer (Fig.1 and Fig.2).

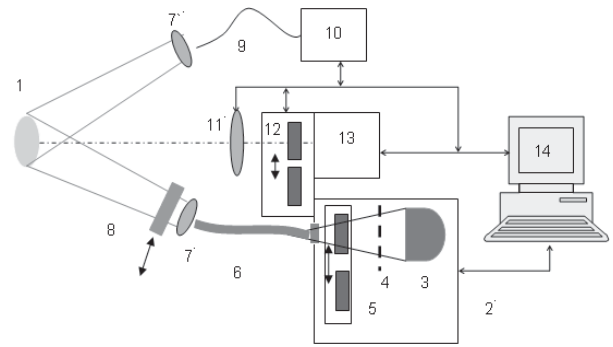


Fig. 1. LuxCol functional diagram. 1 Object, 2 - Illuminator, 3 - mercury lamp, 4 - optical attenuator 5 - replacement color filters, 6 Silica waveguide, 7 - projection lens, 8 - polarizing filter, 9 Liquid-filled waveguide, 10 - laser, 11 - lens, 12 - node of detector assembly replacement filters, 13 - Video Camera, 14 - PC

The registration unit includes the projection lens, the set of detector filter and the digital video camera. Lens focal length is 100 mm and relative aperture $F / 2,8$. Digital video camera is based on the CCD detector (format 2/3 inch) with progressive scan (ICX285AQ, SONY) Maximum frame rate of the camera is 15 Hz at resolution 1280x1024 elements. Its own noise is about $10e^{-}$, non-linearity characteristics of the light signal at differences of light is 100 times less than 3.5%. Signals received from the camera transmit to the computer by the serial high-speed, working according USB-2.0 protocol.

Illuminator is separated into three parts: mercury lamp, halogen lamp and 635nm laser. Excitation power density (mw/cm²) are 26 (360nm), 69 (390nm), 73 (430nm), 170 (635nm) respectively at the view field of 20.8x26 (VxH) mm and the working distance of 220 mm.



Fig. 2. Device LuxCol

B. Clinical study and data set

For algorithm design and their experimental testing we used the real images obtained in 3 hospital of South Korea. Eligible patients were at least 18 year old, not pregnant, were referred to the colposcopy clinic with an abnormal Pap smear or with positive HPV. Written informed consent was obtained from each participant. For all patients we have results of PAP smear and results of HPV test. For researches the set of images were acquired with the device LuxCol from each patient. A set of images was acquired following the application of acetic acid 6% on the cervix for 2-3 min. Finally the diagnose of colposcopist, cervix image with marked points where biopsy was taken and results of biopsy were obtained for each patient. Thus, for investigation we have:

- the sets of images obtained by LuxCol (images obtained with white light illumination (mode 1) and with polarized white light (mode 2); fluorescence image obtained by excitation at wavelength of 360nm (mode 3), 390nm(mode 4), 430nm(mode 5) and 390nm with 635 nm laser(mode 6));
- results of Pap-smear and HPV;
- the diagnose of colposcopist;
- the points of biopsy and result of biopsy for these points.

The total quantity of images set is 123 among them images with CIN - 51, with CNI - 72. These verified set of images we used for creating special data base of records, which is necessary for classifier training. According to verified images with marked points where biopsy was taken we put markers on the images received by LuxCol with white light illumination and the vector of color and brightness features for block of 20 * 20 elements around the marker was calculated with the assistant special program RSS Colpo. This process is illustrated in Fig. 3. Each such image block and its corresponding features vector we called as record in data base. In this way we obtained data base including records, corresponded to norm, CNI and CIN for father investigation.

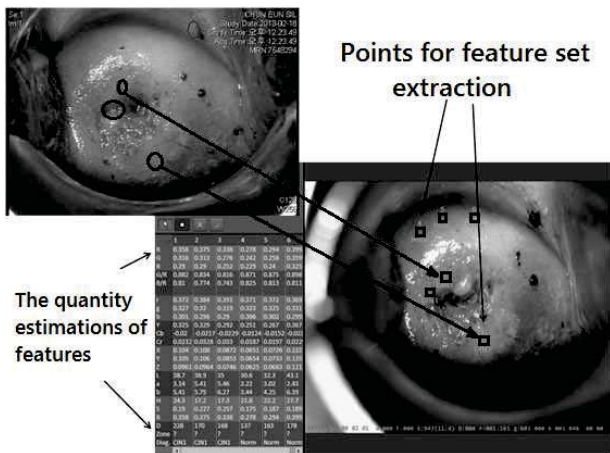


Fig. 3. The feature extraction and estimation (image in the left top corner is verified by biopsy results; image in right bottom corner obtained with Luxcol and we marked points for classificatory training)

We used this special data base of records in next investigations:

- for the most effective mode of images and features selection;
- for the algorithms of preprocessing checking;
- for classifier training;
- for estimation the main characteristics of proposed algorithm such as specificity, sensitivity and accuracy;
- for pathology map creation and its control.

III. BASIC CONCEPTS OF ALGORITHMS

A. Image preprocessing

The effectiveness of medical image analysis is strong connected with their preprocessing. Standard preprocessing includes procedures to improve the quality of the images such as gamma correction, noise reduction, color balance, contrast enhancement, etc. Additional for medical image it is necessary to use special preprocessing procedures such as: automatic regions of interest (ROI) segmentation; removing highlights in the images; and in the case of using multi-spectral fluorescent images procedure of their matching.

The images from different modes may have discrepancy in the coordinates, so called shifts. Large shifts between images can noticeably confuse further analysis so the compensation of the shifts between images in different modes must be realized before tissue classification.

The compensation of the shifts between images of different modes based on phase correlation. We compute the cross-power spectrum of analyzing and reference images.

$$R = \frac{\mathbf{G}_a \circ \mathbf{G}_b^*}{\mathbf{G}_a \mathbf{G}_b^*}$$

where \mathbf{G}_a - the result of Discrete Fourier Transformation of analyzing image, \mathbf{G}_b - the result of Discrete Fourier Transformation of the reference image, \circ - Hadamard matrix multiplication. Then, we calculate the cross-correlation function of images $r(x, y)$ using the inverse Discrete Fourier Transform.

$$r(x, y) = F^{-1}\{R\}$$

The maximum of cross-correlation function determines the spatial displacement between reference and analyzing images:

$$\Delta x, \Delta y = \max_{x, y} (r(x, y))$$

The main advantage of the proposed approach in comparing with the modern algorithms operating in the signal domain is the possibility of matching the images which have significantly different one from another in brightness and color, as well as resistance to noise, occlusion, and similar negative factors of medical images.

Fig. 4 shows the result of the algorithm: the left column shows the initial images obtained in different modes, the right - the image after displacement calculation and compensation.

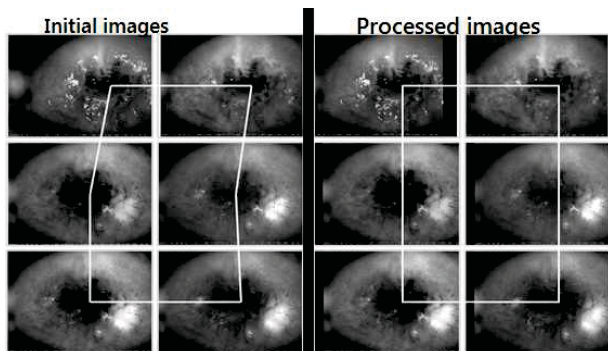


Fig. 4. Shift compensation algorithm results

The sufficient displacements were eliminated during processing.

On a real medical image the image of cervix takes only about 70%. The rest part of image may include other tissue, medical instruments, various artifacts. The presence of irrelevant information makes difficult the further data processing and analysis, so it is necessary to select only the image area corresponded to cervix - the region of interest.

For automatic region of interest segmentation (Fig.5) we proposed the algorithm based on *K*-means clustering in chromaticity layer *a* from Lab color space.

B. Features and classification rule

The main part of cervix multi-spectral image processing is the classification task. To solve classification task it is necessary to choice features for classification and classifier strategy.

There are three groups of pathology signs in the cervix image: brightness and color features, morphological features and texture feature. In current investigation we used for analysis the brightness and color features of image.

To quantify the brightness and color features initial R, G, B coordinates, ratio G / R and G / B, and r g b, XYZ, YCrCb, Lab and HSV coordinates have been used. To reduce the effect of noise all features were calculated for the local fragment - the image block size 20 * 20 and further the average value was used.

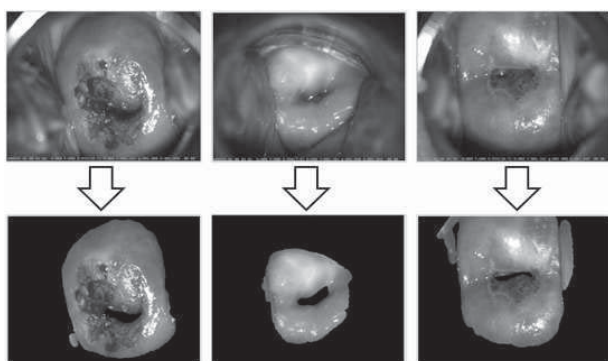


Fig. 5. Results of ROI selection

For the most effective features image modes selection and for pathology map construction the Fischer Distance between classes CIN and CNI was calculated.

$$K_D = \frac{(\bar{x} - \bar{y})^2}{s_x^2 + s_y^2}$$

where \bar{x}, \bar{y} - mean and s_x, s_y variance of feature under investigation for CIN class and CNI class.

According the Fischer Distance between classes CIN and CNI we got next results:

- the most informative is image obtained by excitation with wavelength of 360nm;
- the most effective features in 360 mode are Cr, Cb from YCrCb system and b from Lab system;
- the additional mode for improving classification is 390 mode;
- the most effective features in 390 mode are Cr, Cb from YCrCb system and b from Lab system.

Thus, for classification task we used next set of features: Cr, Cb (YCrCb system) and b (Lab system) calculated in fluorescent images obtained by excitation with wavelength of 360nm and 390nm.

To select the most appropriate strategy for the classification task we used next set of classifiers: the classification based on Mahalanobis metric (linear discriminate analysis, quadratic discriminate analysis); the classification based on regression model (linear multinomial regression, logit regression); Support vector machines; PCA (Principle Component Analysis) with classification by SIMCA (Soft Independent Modeling of Class Analogy); Random decision forest; ADA Boost; Neural networks; the classification based on fuzzy logic.

For classifier training and testing we used approach Leave-one-out cross-validation. Leave-one-out cross - validation involves using a single data point from the original set as the validation data, and the remaining points as the training set. This is repeated such that each point in the set is used once as the validation data.

The most interest and the most difficult for design task is the task of classification CNI and CIN. This task is also the most actual in physician practice. The task of classification CIN/Norm is rather simple and it is not actual for medicine practice. So at first we calculated the specificity, sensitivity and accuracy on the border CIN/CNI. Training and validation of classifier was realized on the data base of records.

Our investigation shows that the best specificity, sensitivity and accuracy are obtained by using Random Decision Forest [18]. The results of RDF classification for the border CNI/CIN obtained on the data base of records with validation approach Leave one-out-cross are next the sensitivity is 0.85, the specificity is 0.78. Additionally we estimate specificity and sensitivity on the border Norm/CNI. The results for the border Norm/CIN : the sensitivity is 0.95, the specificity is 0.90.

Thus, for differential pathology map creation the classification is performed in mode 360 and 390 on the features Cr, Cb from system YCrCb and b from system Lab. The classification strategy is RDF - Random Decision Forest.

C. The algorithm of pathology map creation

The main task for pathology map creation is image classification in three class: Norm, CNI and CIN according strategy and features chosen above. But besides the classification with the aim of differential diagnostic the pathology map creation demands preliminary classification to select columnar epithelium and artifacts. Because these parts must be eliminate from further analysis. Thus in our algorithm we use two stages of classification.

On the first stage we use 2-class RDF classifier for preliminary classification. We realized the features and the modes selection for this task on the base of Fisher distance and obtained that the most effective features are white mode and mode 360 with the features a and b in the system Lab.

On the second stage we use 3-class RDF classifier to separate Norm, CNI and CIN. We use the features Cr, Cb from YCrCb system and b from system Lab for modes 360 and 390. The 3-class RDF classifier means that we have three training samples with examples of all classes. For each one the RDF response is a vector of probabilities of belonging to each class. According to our goal - the pathology map creation, we use this probabilities to define for the current example the membership degree to each class and to color the corresponded block on the output map. Thus, the main steps of differential pathology map creation are:

- the region of interest selection based on the k-means algorithm;
- the compensation of object movement in different modes based on correlation between images in spectral domain;
- the columnar epithelium and artifacts selection based on Random Decision Forest - RDF . The classification is performed in white mode and mode 360 on the features a and b in the system Lab;
- the image blocks three class classification (norm , chronic inflammation CNI, CIN performed in mode 360 and 390 on the features Cr, Cb in system YCrCb and b in system Lab. Classification strategy is RDF - Random Decision Forest;
- the color of differential pathology map blocks corresponding to image blocks is determined on the base RDF response. If the membership degrees of current block to each class for are P_{NORM} , P_{CNI} , P_{CIN} . Then for the color definition (for three component 24 bpp RGB color) we use the following logic.

$$if (P_{NORM} \leq P_{CNI}) and (P_{NORM} \leq P_{CIN}), then$$

$$\begin{cases} R = 255 \cdot (P_{CNI}/(P_{CNI} + P_{CIN})) \\ G = 255 \\ B = 0 \end{cases}$$

$$if (P_{CIN} \leq P_{NORM}) and (P_{CIN} \leq P_{CNI}), then$$

$$\begin{cases} R = 255 \cdot (P_{CNI}/(P_{CNI} + P_{NORM})) \\ G = 255 \\ B = 0 \end{cases}$$

$$if (P_{CNI} \leq P_{NORM}) and (P_{CNI} \leq P_{CIN})$$

$$and (P_{NORM} \leq P_{CIN}), then$$

$$\begin{cases} R = 255 \cdot (P_{CIN}/(P_{CIN} + P_{NORM})) \\ G = 0 \\ B = 0 \end{cases}$$

$$if (P_{CNI} \leq P_{NORM}) and (P_{CNI} \leq P_{CIN})$$

$$and (P_{CIN} \leq P_{NORM}), then$$

$$\begin{cases} R = 0 \\ G = 255 \cdot (P_{NORM}/(P_{CIN} + P_{NORM})) \\ B = 0 \end{cases}$$

IV. RESULTS

The experimental investigation of proposed algorithm includes two part. The first part realized classifier validation. It was performed on the data base of record with the strategy Leave-one-out-cross. The obtained result on the border CNI/CIN sensitivity is 0.85, the specificity is 0.78. But the main part of the experimental research is the pathology map obtaining and estimation (Fig. 6).

For this investigation at first we divided all images of cervix with biopsy results in two groups. If image has at least one biopsy with diagnosis CIN (each image can have several points with biopsy), then this image belongs to the class CIN. If for image there are no biopsy with result CIN, all biopsies have result CNI then image belongs to class CNI.

The investigation includes next steps.

- 1) According data base of record with Leave-one-out-cross approach the classifier training was realized.
- 2) For image, which records were eliminate from training the pathology map was created. The pathology map indicates three classes Norm, CNI and CIN. In the pathology map the cervix areas belonging according classification results to Norm have green color, the areas with CNI have yellow color and the areas with CIN have red color. If area of cervix has intermediate state, for example, between Norm and CNI, its color is the mix of pure colors corresponded these diagnosis. The percentage of pure color in mixing color corresponds to the severity of each tissue states (diagnoses). So, in our example Norm/CNI area will be have color including green and yellow. If state of tissue is intermediate between CNI and CIN then color of area in the pathology map will be mix of red and yellow.
- 3) The obtained pathology map was checked according biopsy results in next way. If results of classification was CIN and the image belongs to class CIN, then we increment TP (true positive) value. If the results of classification was CIN, but image belongs to class CNI, then we increment FN (false negative) value. If results of classification was CNI and the image belongs to CNI, then we increment TP (true positive) value. If results of classification was CNI but the class of image was CIN, then we increment FP (false positive) value.

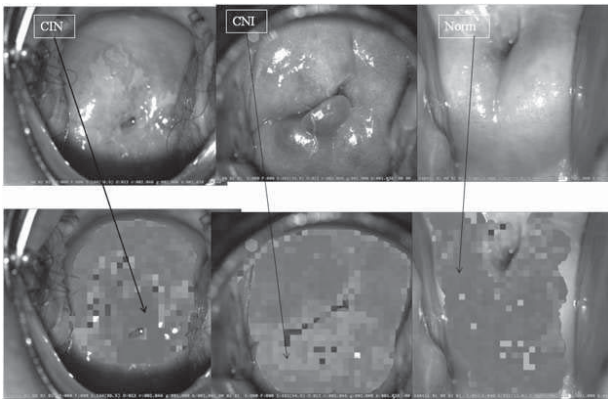


Fig. 6. Examples of pathology map with 3 classes Norm, CNI and CIN

Steps 1-3 were repeated for all images under investigation and according to results we estimate the main classifier characteristics (accuracy, sensitivity and specificity) base on obtained pathology maps. The results are given in Table I.

$$accuracy = \frac{TP + TN}{TP + FP + TN + FN}$$

$$sensitivity = \frac{TP}{TP + FP}$$

$$specificity = \frac{TN}{TN + FN}$$

TABLE I. RESULTS

LuxCol				Characteristics of LuxCol		
CNI		CIN		Border Norm+ CNI/ CIN		
True according to histology	Total	True according to histology	Total	Sensitivity	Specificity	Accuracy
51	72	44	51	0.87	0.71	0.78

From Table I you can see that accuracy of proposed method on the border CNI/CIN is 0.78. Examples of obtained pathology map are given in figures 6,7. The Fig. 7 demonstrates that points with biopsy result CIN are corresponded dark (red in color image) areas in obtained pathology map.

V. CONCLUSION

Analysis of fluorescence images obtained by excitation with wavelength of 360 and 390 nm allows to detect follow states of cervix tissues Norm, CNI, CIN. For the border CIN/CNI we got sensitivity 83% and specificity 72% (leave-one-out-cross validation).

These figures correspond to estimates of sensitivity and specificity for colposcopic examination conducted by an experienced physician and exceeds characteristics of inexperienced physician, where the sensitivity and specificity have been reported [4] to range from 87 to 96% and 48 to 85%. The essential feature of the developed algorithms is the pathologies maps obtaining. In this map the degree of pathology confirming is obtained for each area of cervix image.

Maps based on three main classes Norm, CNI and CIN. It is important that the classification border CIN/ CNI is realized, because it is the most difficult for medicine practice case.

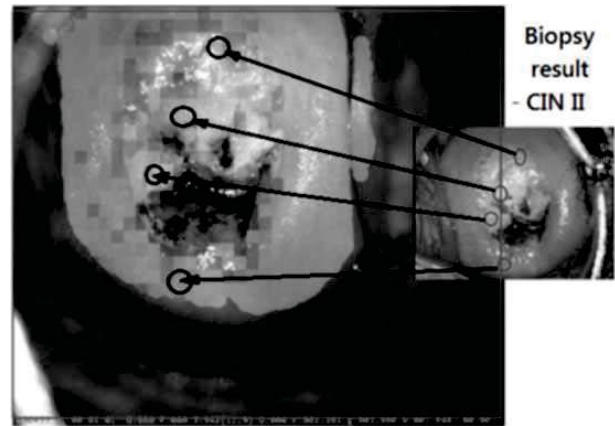


Fig. 7. Corresponding of biopsy points with diagnose CIN II to dark areas of pathology map. Note that the builded map is correct in accordance with results of biopsy points

These maps can be used directly for colposcopist examination or for implementing so-called optical biopsy.

In the last case it is assumed that the physician specifies a certain area of the image, and receives a numerical estimation of pathology confirming degree for this area.

Proposed algorithms gives possibility to obtain correct differential pathology map with probability 0.8 (sensitivity 87% and specificity 71%). Obtained results and classification task characteristics shown possibility of practical application pathology map based on fluorescents images.

In our current work we used images obtained in white light for the columnar epithelium and artifacts selection based on Random Decision Forest - RDF. An additional direction of research the authors suggest the combination of the proposed approach with analysis of the colposcopic images obtained in white light illumination, in particular, acetowhite areas detection and the texture estimation.

REFERENCES

- [1] H.H. Chung, M.J. Jang, "Cervical cancer incidence and survival in Korea: 1993-2002", *International Journal of Gynecological Cancer*, vol.16/5, 2006, pp. 1833-1838.
- [2] L.G. Koss, "The Papanicolaou test for cervical cancer detection: a triumph and a tragedy", *J. Am. Med. Assoc.*, vol.261, 1989, pp. 737-743.
- [3] M.F. Mitchell, D. Schottenfeld, "Colposcopy for the diagnosis of squamous intraepithelial lesions: a meta-analysis", *Obstet. Gynecology*, vol.91, 1998, pp. 626-631.
- [4] S. Yang, J. Guo, "A multi-spectral digital cervigramTM analyzer in the wavelet domain for early detection of cervical cancer", *Proceedings of SPIE on Medical Imaging*, vol.5370, 2004, pp. 1833-1844.
- [5] S. Gordon, G. Zimmerman, H. Greenspan, "Image segmentation of Uterine Cervix images for indexing in PACS", *Symposium on Computer-Based Medical Systems*, Bethesda, Maryland, June, 2004, vol.91, pp. 1-6.
- [6] J. Xiong, L. Wang, J. Gu, "Image Segmentation of the Acetowhite region in Cervix Images Based on Chromaticity", *Proc. of 9 Int. Conference on Information Technology an Applications in Biomedicine*, 2009, pp. 1-4.
- [7] X. Huang, J. Engel, "Tissue Classification using Cluster Features for Lesion Detection in Digital Cervigrams", *SPIE Medical Images*, 2008, pp. 69141Z.1-69141Z.8.

- [8] J. Qiang, J. Engel, E. Craine, "Texture Analysis for classification of Cervix Lesions", *IEEE Transactions on Medical Imaging*, vol.19/11, 2000, pp. 1144-1149.
- [9] J. Qiang, J. Engel, E. Craine, "Classifying cervix tissue patterns with texture analysis", *Pattern Recognition*, vol.33, 2000, pp. 1561-1573.
- [10] C. Balas, "A novel optical imaging method for the early detection, quantitative grading, and mapping of cancerous and precancerous lesions of cervix", *IEEE Transactions on Biomedical Engineering*, vol.48/1, 2001, pp. 96-104.
- [11] M. Irene, G. Orfanoudaki, C. Themelis, "A clinical study of optical biopsy of the uterine cervix using a multispectral imaging system", *Gynecologic Oncology*, vol.96, 2005, pp. 119-131.
- [12] I. Claude, R. Winzenrieth, "Contour Features for colposcopic image classification by artificial neural networks", *Proceedings of international conference on Pattern Recognition*, vol.96, 2002, pp. 771-774.
- [13] P. Mitra, S. Mitra, "Staging of Cervical Cancer with Soft Computing", *IEEE Transactions on Biomedical Engineering*, vol.47/7, 2002, pp. 934-940.
- [14] A. K. Dattamajumdar, D. Wells, "Preliminary experimental results from multi-center clinical trials for detection of cervical precancerous lesions using the CerviscanTM system: a novel full field evoked tissue fluorescence based imaging instrument", *Proceedings of the 23rd Annual EMBS international conference*, 2001, pp. 3150-3152.
- [15] J.M. Benavides, S. Chang, "Multispectral digital colposcopy for in vivo detection of cervical cancer", *Optics express*, vol.11/10, 2003, pp. 1223-1236.
- [16] S. Park, K. Sokolov, "Multispectral digital microscopy for in vivo detection of oral neoplasia in the hamster cheek pouch model of carcinogenesis", *Optics express*, vol.13, 2005, pp. 749-762.
- [17] S. Park, M. Follen, "Automated image analysis of digital colposcopy for the detection of cervical neoplasia", *Biomedical Optics*, vol.13, 2008, pp. 14-29.
- [18] L. Breiman, "Random Forests", *Machine Learning*, vol.45, 2001, pp. 5-32.